Final Report *February 1980*

LIDAR DETERMINATION OF THE COMPOSITION OF ATMOSPHERIC AEROSOLS

By: M. L. WRIGHT

Prepared for:

NATIONAL AERONAUTICS AND SPACE ADMINISTRATION
AMES RESEARCH CENTER
MOFFETT FIELD, CALIFORNIA 94035

NASA CONTRACT NAS2-10126

SRI Project 8127

SRI International
333 Ravenswood Avenue
Menlo Park, California 94025
(415) 326-6200
Cable: SRI INTL MPK
TWX: 910-373-1246

SRI International

SRI International

Final Report *February 1980*

LIDAR DETERMINATION OF THE COMPOSITION OF ATMOSPHERIC AEROSOLS

By: M. L. WRIGHT

Prepared for:

NATIONAL AERONAUTICS AND SPACE ADMINISTRATION
AMES RESEARCH CENTER
MOFFETT FIELD, CALIFORNIA 94035

NASA CONTRACT NAS2-10126

SRI Project 8127

Approved by:

CHARLES J. SHOENS, *Director*
Systems Techniques Laboratory

DAVID A. JOHNSON, *Executive Director*
Technology and Systems Development Division

SRI INTERNATIONAL, 333 Ravenswood Avenue, Menlo Park, California 94025
(415) 326-6200, Cable: SRI INTL MPK, TWX: 910-373-1246

SRI International

ABSTRACT

This report describes the work that has been done on a project to determine the feasibility of using a DIfferential SCatter (DISC) lidar system to measure the composition of atmospheric aerosols. This report also contains a brief summary of both the theoretical and experimental investigations that were presented in greater detail in previous reports. Part of this work was done on a previous contract but is included here to provide a complete description of the entire effort.

The first tasks in this effort were theoretical investigations of the DISC technique. This theoretical effort indicated that the technique could be useful in measuring the composition of stratospheric aerosols, and led to a series of experiments using a CO lidar system. Early experimental measurements indicated that the signal-to-noise ratios (SNR's) obtainable for stratospheric aerosols would be too low to permit a stratospheric DISC measurement to be made. Instead, a revised experiment involving simultaneous measurement of cirrus clouds and tropospheric aerosols was substituted for the original stratospheric measurements. These two targets had sufficient SNR to permit scatter measurements to be made.

Large variations in cirrus cloud density, and thus pulse-to-pulse backscattered power, made it necessary to change both the theoretical analysis procedures and the experimental apparatus. These changes were necessary because it was not possible to provide an absolute power reference or calibration for each wavelength used in the measurement. Instead, a second laser operating at a fixed wavelength was used to provide a correction for the variations in cirrus cloud

density. This change in reference forced a change in the theoretical analysis procedures, and the new procedures are described in the report.

Extensive changes in the lidar system were made during the course of the experiments. A second laser transmitter was added to provide a power calibration for the system. Hardware and software changes were made in the data acquisition system in order to accommodate the new data format and analysis procedures. Extensive shielding and wiring modifications were made to eliminate the electromagnetic interference (EMI) that prevented high-altitude signals from being observed in the early experimental measurements. Additional modifications are described in the report.

The modified system was able to successfully measure differential backscatter spectra for tropospheric aerosols and cirrus clouds. The experimentally-observed backscattering ratios were closest to the calculated backscattering ratios for water and ice, although significant discrepancies existed at the longer wavelengths. Corrections for atmospheric attenuation, temperature dependence of refractive index, and other parameters were made but did not reduce the apparent discrepancy between the experimental measurements and the theoretical calculations. The effects of non-spherical particles or mixtures of materials were not investigated but could be responsible for the discrepancy.

The original estimates of system performance indicated that it would be possible to detect signals backscattered from stratospheric aerosols. However, the modifications made to the experimental apparatus, in order to permit wide-wavelength tuning for the tropospheric and cirrus measurements, reduced the system sensitivity to the point where stratospheric aerosols could no longer be observed. Also, the original backscatter estimates were made for a time period immediately following a volcanic eruption. The reduction in backscatter for the present non-volcanic conditions would also make the detection of stratospheric aerosols more difficult. An analysis

of the sensitivity expected with the present experimental lidar system is presented.

An analysis of the performance capabilities of a lidar system for the space shuttle is also presented. This system is capable of detecting tropospheric aerosols and subvisible cirrus clouds but would be marginal for stratospheric aerosols during non-volcanic times unless larger lasers are used. Although larger lasers systems are now commercially available, the limitations would seem to be in the large primary power sources necessary to run these systems on a continuous basis.

CONTENTS

ILLUSTRATIONS

TABLES

I INTRODUCTION

In recent years there has been a growing concern that major changes in aerosol content of the earth's atmosphere could alter global radiation balance and thus produce significant changes in the earth's mean surface temperature. Either natural or anthropogenic causes could produce perturbations large enough to lead to the initiation of a minor or a major new ice age. Increasing industrial, agricultural, and aerospace activities, along with natural volcanic activity, may lead to increases in tropospheric and stratospheric aerosol concentrations. Particulates produced by emissions from supersonic transports, space shuttles, and large volcanic eruptions affect the aerosol content of the stratosphere. Stratospheric aerosols may have a global effect on radiation balance and climate because of the aerosol's long residence time; these aerosols are the focus of a major part of the concern.

It is important to define the chemical composition of the current atmospheric aerosols and to be able to monitor changes in the chemical composition of the aerosols at various altitudes, including the stratosphere, to model the effects of these changes. Collection experiments have helped meet this need to a certain extent; however, because the samples are collected under one set of conditions and examined under another, some of the materials, particularly relatively volatile compounds such as sulfuric acid, may be significantly altered by the time samples are analyzed. Therefore, it is desirable to have a remote sensing method of determining aerosol composition.

A remote sensing system capable of determining the chemical composition of atmospheric aerosols also would be desirable in that it could reduce the cost of long-term measurements, especially in the stratosphere, and avoid some of the difficulties encountered in aerosol sampling systems. Moreover, a remote sensing system could allow aerosol measurements to be made at altitudes in the stratosphere that are beyond the reach of most aircraft. Lidar (laser radar) remote sensing systems can provide simultaneous information on the variation of composition with altitude. Such a system operated from a satellite might be able to provide atmospheric aerosol measurement capability.

This report summarizes the theoretical and experimental work that has been done to investigate the feasibility of making remote measurements of the chemical composition of atmospheric aerosols by means of the differential-scatter (DISC) lidar technique. This technique uses characteristic differences in the infrared backscatter spectra of aerosols to identify their chemical composition. The DISC technique for aerosols is an extension of SRI's extensive work with laser systems designed to measure the composition of atmospheric gases. The work summarized in this report has led to the conclusion that the DISC system can, under some conditions, measure the chemical composition of atmospheric aerosols. Part of this work was done on a previous contract but is reported here to present a complete description of the effort.

II EXPERIMENTAL WORK

A. Background

The first part of this system includes work done on both this contract and a previous contract in order to provide a complete description of the DISC effort to date.

The chemical composition of atmospheric aerosols varies both in time and space. Not only will stratospheric aerosols be different from tropospheric aerosols, but the chemical composition of stratospheric aerosols may change following a major volcanic eruption. Remote measurements of aerosol composition can provide valuable information for studies of aerosol transport and chemistry.

SRI began studying the dependence of the scattering properties of aerosols on chemical composition as an outgrowth of work on lidar systems to measure the chemical composition of atmospheric gases. The results of this investigation indicated that the scattering properties of aerosols are dependent on the chemical composition of the aerosol. In particular, the backscattering spectrum of an aerosol was found to have characteristic spectral features that could be used to identify the chemical composition of the atmospheric aerosol. A similar investigation was carried out independently by Dr. James Pollock, at NASA Ames Research Center. The NASA work was oriented toward measuring the chemical composition of aerosols on distant planets and studying both long and short-term changes in the composition of stratospheric aerosols. A common interest between SRI and NASA in remote measurement of aerosol composition led to a cooperative effort to study the feasibility of building lidar instruments to measure the

chemical composition of atmospheric aerosols, with particular emphasis on stratospheric aerosols.

1. Spectral Characteristics of Backscattering

The distinctive nature of backscattering spectra for different aerosols is shown in Figure 1[1*]. This figure shows the relative volume backscatter coefficient for five different materials that are associated with stratospheric or atmospheric aerosols. The particle size distribution for the spectra shown in Figure 1 are appropriate for stratospheric aerosols.

One reason for choosing stratospheric aerosols was to minimize the effect of aerosol size on the backscattering spectra. Stratospheric aerosol particles are small compared to the wavelengths that would be used for composition measurements. Particle size effects will begin to occur when the particle size becomes comparable to the probing wavelength. At this point, electromagnetic resonances in the particle can alter the scattering properties significantly. Since these resonances are wavelength-dependent, the size effects can produce spectral features that can mask the spectral features caused by the chemical composition of the particle. Particle size resonance effects will also disappear when the particle becomes sufficiently large if the particle size distribution is moderately wide. The range of particle sizes for which resonance effects will be significant depends on the probing wavelength, the particle composition, the particle shape, the distribution of composition within the particle, and the surface roughness of the particle.

The wavelength region over which backscattering spectra are likely to exhibit characteristic features extends from one micron to tens of microns. For remote measurements, atmospheric transmission will limit the wavelength range to approximately 14 μ. Fortunately, many chemicals exhibit molecular resonances in this wavelength region.

*References are given at the end of this report

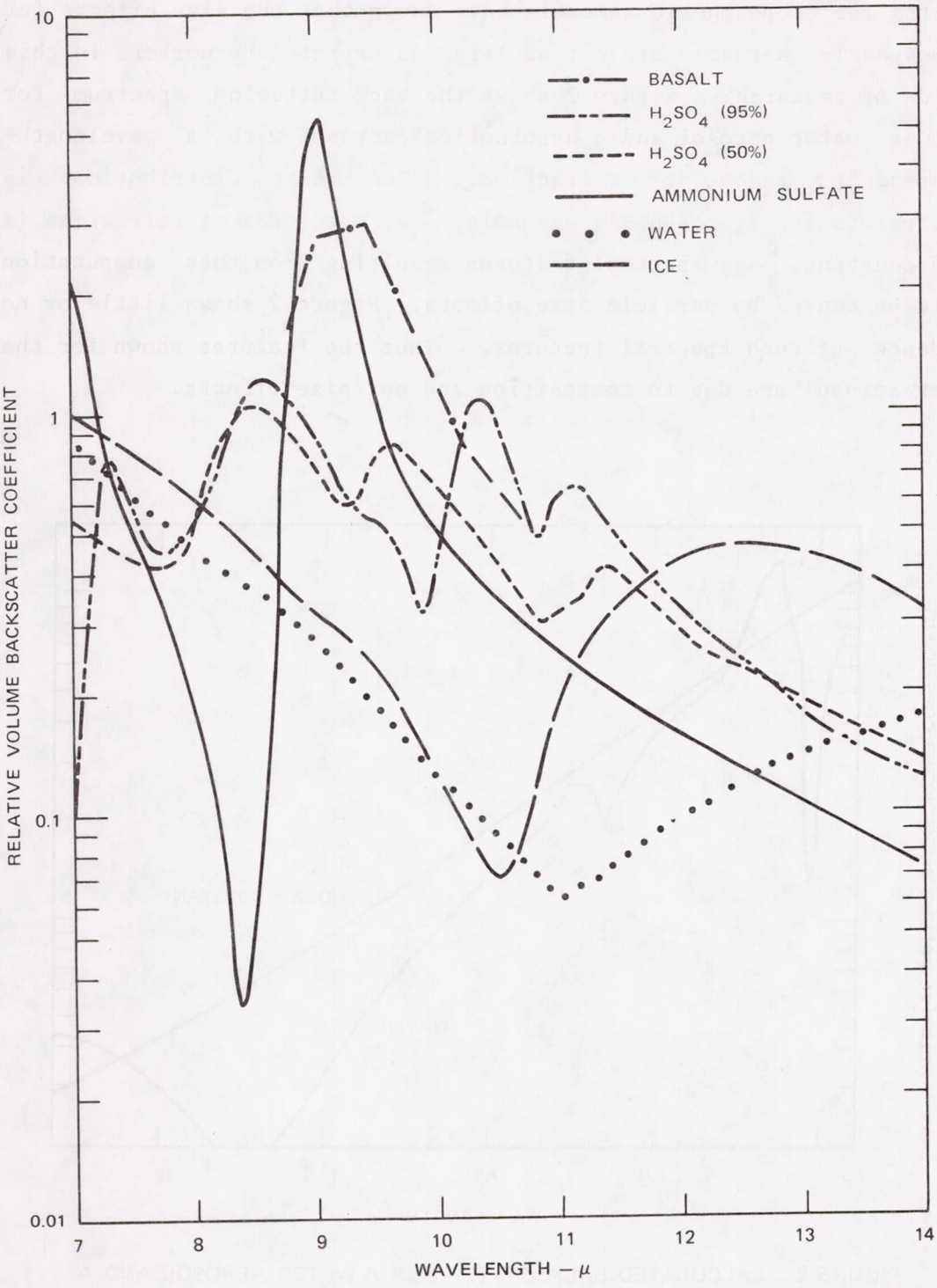

FIGURE 1 RELATIVE BACKSCATTER FOR SEVERAL ATMOSPHERIC AEROSOLS

Recent investigations of particle size effects on backscattering spectra for tropospheric aerosols have shown that the size effects for tropospheric aerosols are not as large as expected by workers in this field of research. Figure 2 shows the backscattering spectrum for both a water aerosol and a hypothetical aerosol with a wavelength-independent index of refraction. The size distribution is appropriate for tropospheric aerosols. If the index of refraction is held constant, any spectral features resulting from this computation would be caused by particle size effects. Figure 2 shows little or no evidence of such spectral features. Thus the features shown for the water aerosol are due to composition and not size effects.

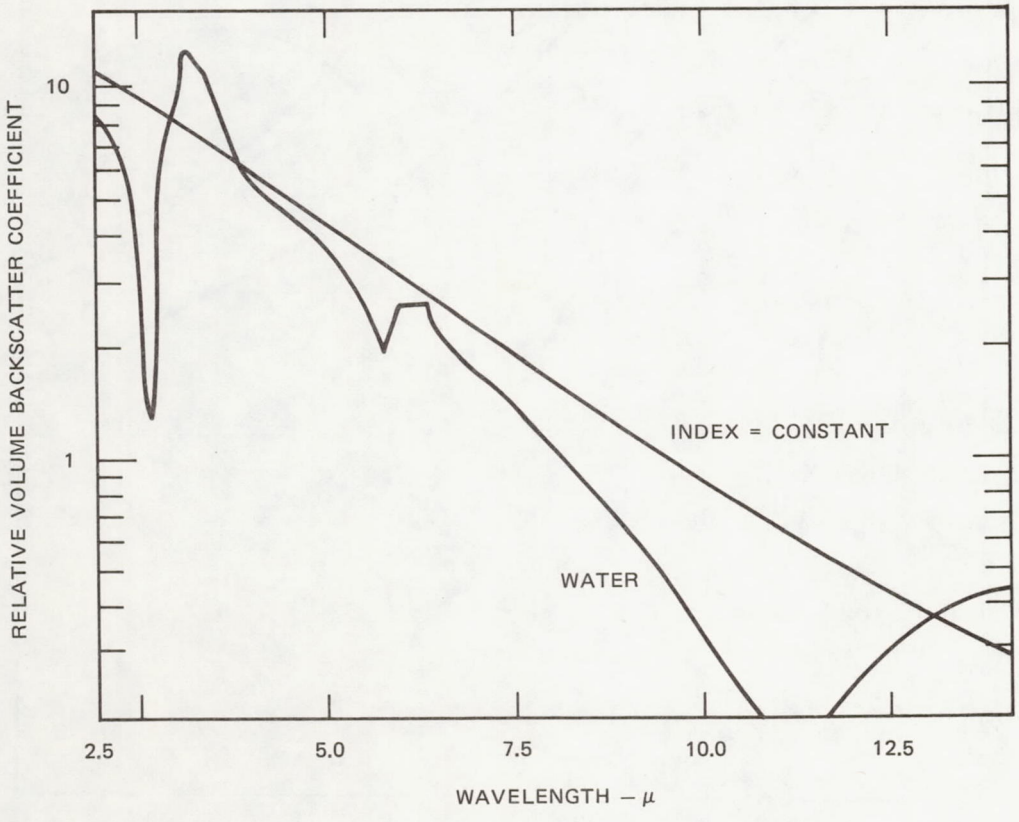

FIGURE 2 CALCULATED BACKSCATTER FOR A WATER AEROSOL AND A HYPOTHETICAL AEROSOL OF CONSTANT INDEX

2. Optimum Wavelength Selection

Once the backscattering spectral characteristics of the aerosol constituent have been determined, the next step is to choose the optimum set of wavelengths for that measurement. Optimum wavelengths are defined as those that permit maximum discrimination among constituents to be made. Pattern recognition techniques are utilized to define discrimination and to perform the discrimination in experiments.

In order to understand the method of choosing the optimum wavelength set, it is helpful to examine how the observations from a DISC experiment would be analyzed. If the volume backscatter coefficient of the atmospheric aerosol is measured at a series of wavelengths, a set of measurements such as those plotted in Figure 3(a) is obtained. Since the aerosol number density is unknown, the measurements give only the relative backscatter coefficient. If we assume that the true backscatter coefficient is one of a set of models as shown in Figure 3(b), then the composition can be determined by pattern recognition or by maximizing the cross correlation between a model and the experimental observations.

It is customary to represent a model, or, in our case, a particular material, as a "feature vector" in a "feature space" whose axes are measurable characteristics of the model.[2] For DISC systems the recognition or classification features are the values of the volume backscatter cross section at a set of selected wavelengths at which the measurements are performed. Thus, each material is represented by a point in an n-dimensional hyperspace.

Selection of an optimum set of wavelengths consists of examining successive sets of wavelengths and finding the set that maximizes the spatial separation of materials in the n-dimensional hyperspace. The actual techniques for maximizing the separation are rather complex and are described in an interim technical report.[3]

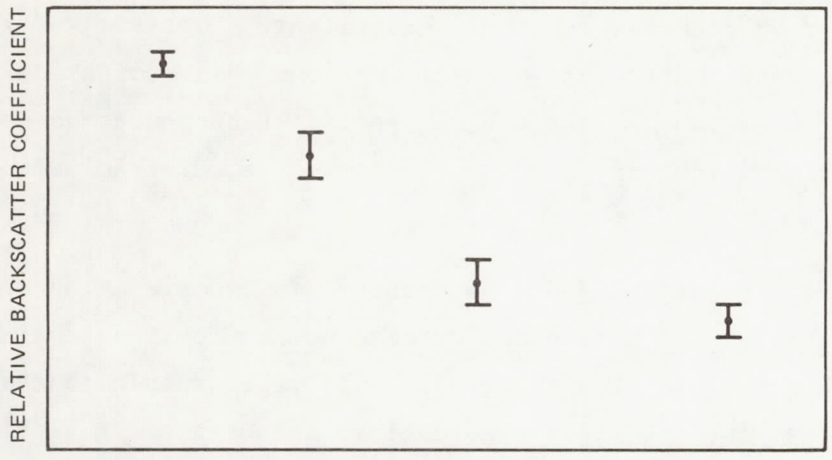

(a) EXPERIMENTAL OBSERVATIONS

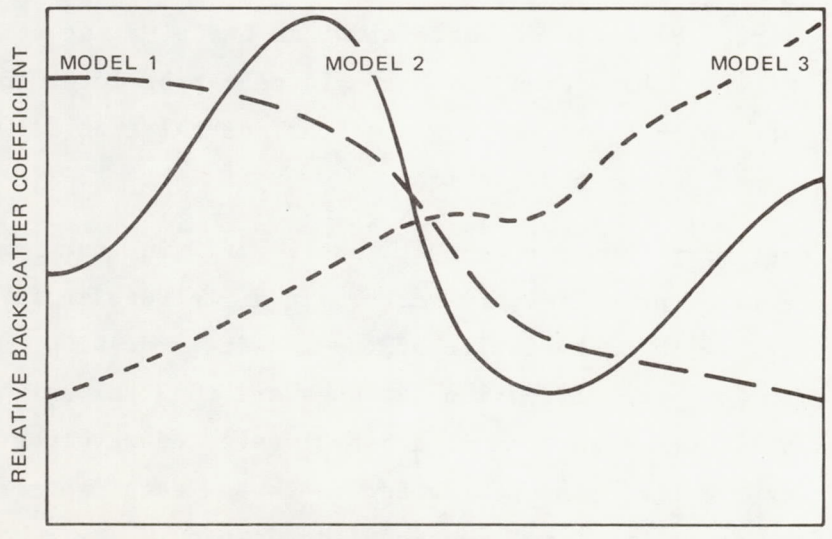

(b) AEROSOL MODELS

FIGURE 3 AN EXPERIMENTAL DATA SET AND SEVERAL POSSIBLE MODELS FOR COMPARISON

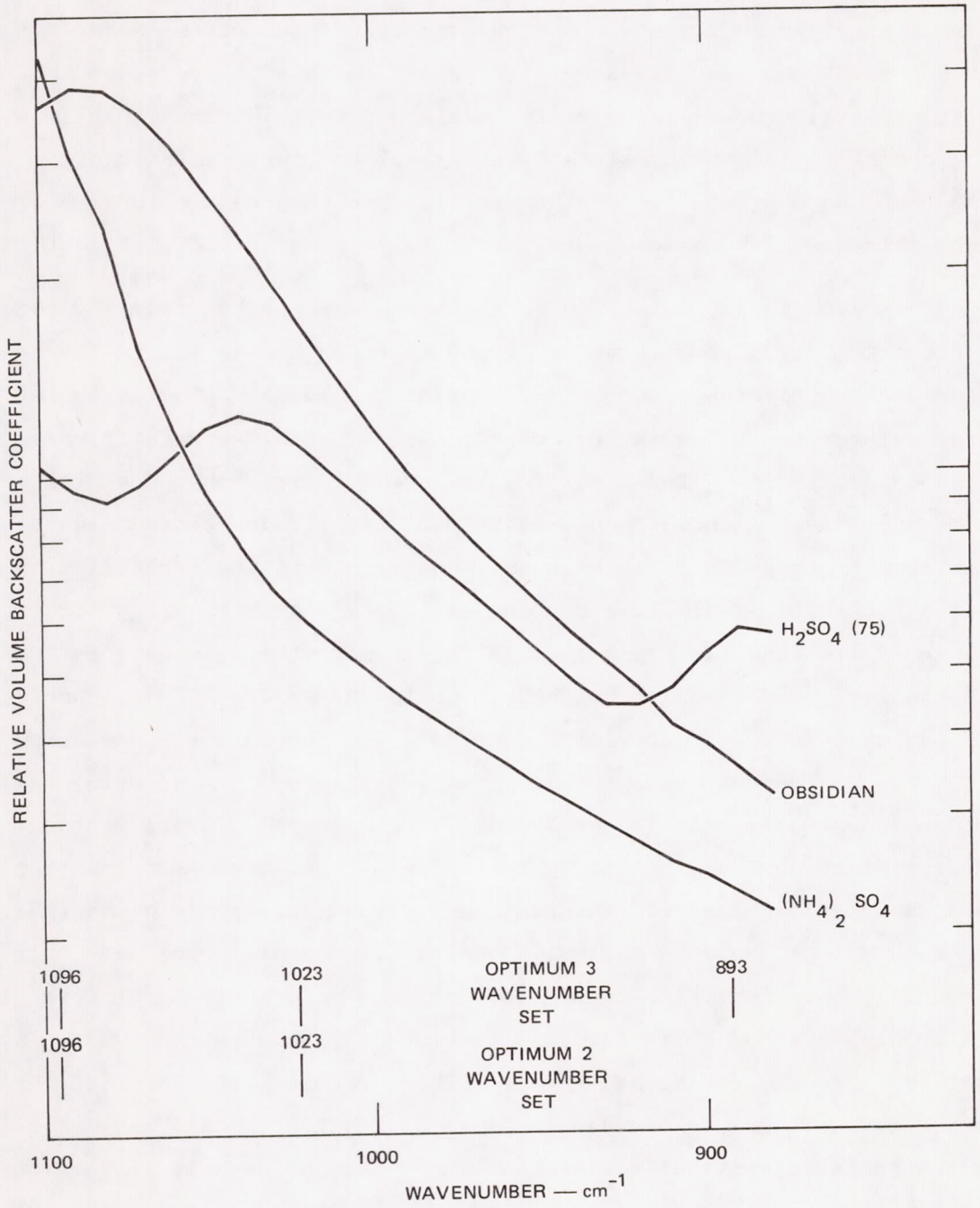

FIGURE 4 OPTIMUM WAVELENGTHS FOR DISCRIMINATION BETWEEN H_2SO4 (75), $(NH_4)_2SO4$, AND OBSIDIAN

The optimum discrimination wavelengths do not necessarily correspond to the wavelengths of characteristic peaks and valleys in the spectra of the materials to be discriminated. Thus an intuitive choice of spectral features would not necessarily lead to an optimum set of wavelengths for maximum discrimination. An example of an optimum wavelength set is shown in Figure 4. This figure shows the wavelength (wavenumber) location for maximum discrimination capability among obsidian, ammonium sulphate, and a 75% sulphuric acid solution. Note that the optimum wavelengths are close to spectral features but do not coincide with these points.

If noise and/or other uncertainties are introduced in the measurement, the discrete points representing each material in the n-dimensional hyperspace become n-dimensional volumes. The size of these volumes can be varied by introducing different amounts of noise and/or uncertainties. For a particular level of error the probability of correct identification and misidentification (false alarm) can be calculated by Monte Carlo techniques. An example of the probabilities of the correct identification and misidentification using this technique is shown in Table 1. In this case, the materials to be distinguished are ammonium sulphate, obsidian, and a 75% sulphuric acid solution. The material assumed to be present is ammonium sulphate. A Monte Carlo trial that identifies the material as ammonium sulphate is considered a correct identification. Misidentification occurs if the Monte Carlo trial results in either obsidian or sulphuric acid. Approximately 1,000 trials are summarized for each case shown in Table 1. For a fractional error of 0.1, essentially no misidentifications occurred. Note that a relatively high probability of correct identification still occurs even with a relative large 0.5 fractional error. These results indicate that the system is not critically dependent on high SNR's, and may still operate satisfactorily at reasonable SNR. Further details regarding probabilities of correct identification and misidentification are given by Wright.[3]

TABLE 1

Probability of Correct Identification	Probability of Misidentification		Assumed Values of the Fractional Error (at Each of Three Wavelengths)
	As H_2SO_4(75%)	As Obsidian	
1.000	0.000	0.000	0.100
0.852	0.006	0.142	0.300
0.728	0.096	0.176	0.500

*Materials to be distinguished: H_2SO_4(75%), $(NH_4)_2SO_4$, and obsidian
Materials assumed to be present: $(NH_4)_2SO_4$.

3. Experimental System Design

The encouraging results of the theoretical studies led to the initiation of an experimental system design for a stratospheric aerosol measurement. A more logical progression towards a final stratospheric measurement might have included a laboratory verification of the scattering properties predicted by the theory. However, the available apparatus was not well suited to a laboratory measurement and funding was not available for construction of the suitable laboratory apparatus. For these and other reasons, laboratory verification was bypassed and an experimental design for a stratospheric measurement was undertaken.

The original experimental apparatus was designed to take advantage of an existing 48-in.-aperture telescope and tunable CO_2 laser already shown in Figure 5. The calculated performance of this system is shown in Table 2. The SNR shown in Table 2 would be high enough to permit measurements of stratospheric aerosols by integrating less than 1,000 shots.

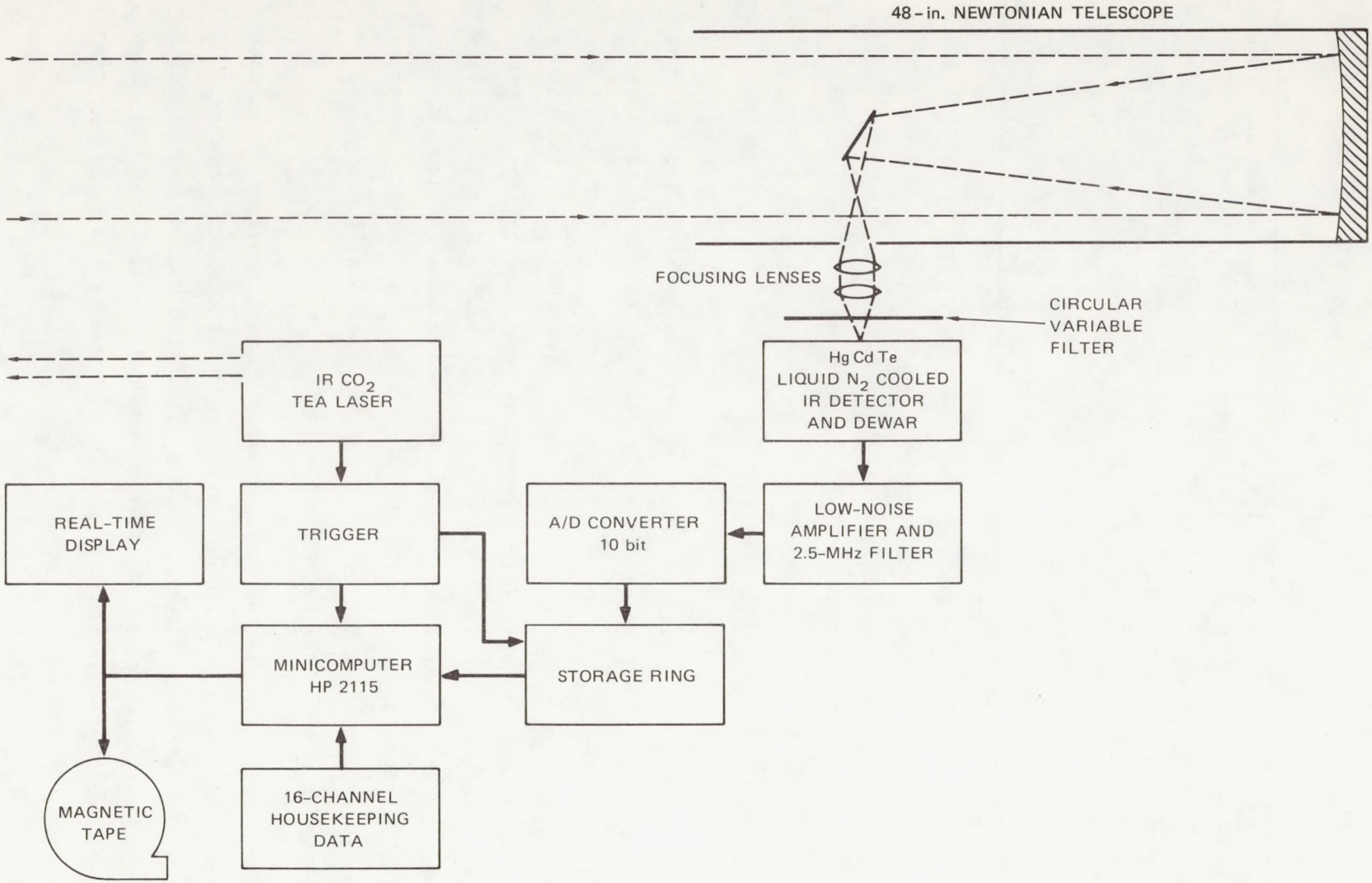

FIGURE 5 EQUIPMENT DIAGRAM FOR THE ORIGINAL EXPERIMENTAL INFRARED DISC LIDAR SYSTEM DESIGN

This encouraging result led to the start of construction of the experimental apparatus. Unfortunately, a number of difficulties were encountered in trying to adapt the existing apparatus for the intended measurement. The first difficulty occurred when the infrared detector manufacturer could not deliver a detector with the promised specifications that had been used for the performance estimates. SRI was forced to use a detector of lower performance, although the difference in detector characteristics alone was not sufficiently large to invalidate the experimental attempt.

TABLE 2

SIGNAL-TO-NOISE RATIOS
EXPECTED FROM THE ORIGINAL
LIDAR SYSTEM DESIGN

Number of Samples Integrated	Signal-to-Noise Ratio of 75% Aqueous Solution of H_2SO_4
1	3
10	9
100	30
1000	94

The second difficulty occurred when it was discovered that the optical quality of the existing 48-in telescope mirror was too low to permit focusing of the received energy on the relative small area of the infrared detector. Various attempts to overcome this difficulty were tried but were unsuccessful. At about the same time, SRI learned of a 36-in. high-quality mirror that might be available from Edgewood Arsenal. Through the efforts of NASA-Ames personnel, this telescope was subsequently made available for use on this project. SRI then

shipped this telescope from Edgewood Aresenal to Menlo Park, and began the task of dismantling and reconstructing the telescope in a configuration suitable for this experiment. This remounting and reconstruction of the telescope utilized the remaining contract funds that were originally earmarked for the stratospheric experiment, and a contract continuation was secured to complete the experiment. Funding was not available to buy the tunable, cooled infrared filter specified in the original system design, and so a cooled, fixed-wavelength filter was substituted for the original design. In order to restrict the background intensity, the filter had a relative narrow bandwidth and thus restricted the tuning range over which the laser could operate. Further changes to the system were caused by the unavailability of the Hewlett-Packard minicomputer that was to be used for data acquisition. Fortunately, a microcomputer was available for the data acquisition and processing. In fact, the improved software for the microprocessor probably reduced software development costs below those which would have resulted from use of the Hewlett-Packard minicomputer.

A series of measurements using this experimental lidar system seemed to produce indications of signal returns from a stratospheric aerosol layer. However, careful examination of the results showed that the apparent signal returns were an artifact of the system. The problem was initially attributed to the overload recovery characteristics of the infrared detector and preamplifier. Insufficient funds remained on the project to permit probing of the equipment problems in greater depth, and the remaining funds were utilized in preparation of a final report.

In summary, the status of the DISC effort prior to the present contract was as follows:

(1) Further work was necessary to complete the construction of an infrared lidar system for stratospheric and/or atmospheric measurements

(2) Adequate SNR's for ground-based measurements of infrared backscatter from stratospheric aerosols appear to be achievable with systems using existing commercially-available hardware. The limitations of the existing laboratory demonstration laser system appear to make stratospheric measurements marginal

The conclusions of the theoretical studies were as follows:

(1) Different stratospheric aerosol materials have significantly different calculated backscattering spectra at infrared wavelengths

(2) Backscatter appears more suitable than extinction for consitituent measurement because of greater "contrast" of spectral features, and because it allows the use of active lidar systems with their relatively unrestricted optical path geometry

(3) Careful selection of operating wavelength is necessary to obtain optimum system performance

(4) Multiple measurement wavelengths will be required, and an optimum number of wavelengths may exist for a particular discrimination experiment

(5) A pattern recognition technique has been developed that appears to have a high probability of correctly identifying single stratospheric aerosol constituents (multiple constituent discrimination has not yet been analyzed).

B. Objective

The objective of this contract was to complete the laboratory-demonstration lidar system and to experimentally demonstrate differential scatter from atmospheric aerosols.

At the beginning of this study, it was recognized by both SRI and NASA-Ames personnel that a multi-wavelength DISC measurement of stratospheric aerosols was an extremely difficult experiment. Also, the measurement was being attempted with a total budget that was smaller than that required for a simpler measurement of gaseous constituents in the troposphere. These two factors give a low probability of making a successful measurement. Nevertheless, a successful DISC measurement of a stratospheric aerosol would pave the way for early implementation of this technique on the Space Shuttle. Unfortunately, a number of experimental difficulties occurred and it appeared that the stratospheric DISC measurements would not be possible within the constraints of available time and funds.

After some discussion between SRI and NASA-Ames, a more feasible DISC experiment was planned. This new experiment involved the simultaneous measurement of tropospheric aerosols and cirrus cloud layers; the objective being to measure the differential backscatter of these two targets. A pictorial representation of this new experiment is shown in Figure 6. The tropospheric aerosol is close to the lidar system and produces a large signal return. The cirrus clouds, although further away, are more dense and not as distant as the stratospheric aerosol layer and thus can also produce measurements with a higher SNR than can stratospheric aerosols.

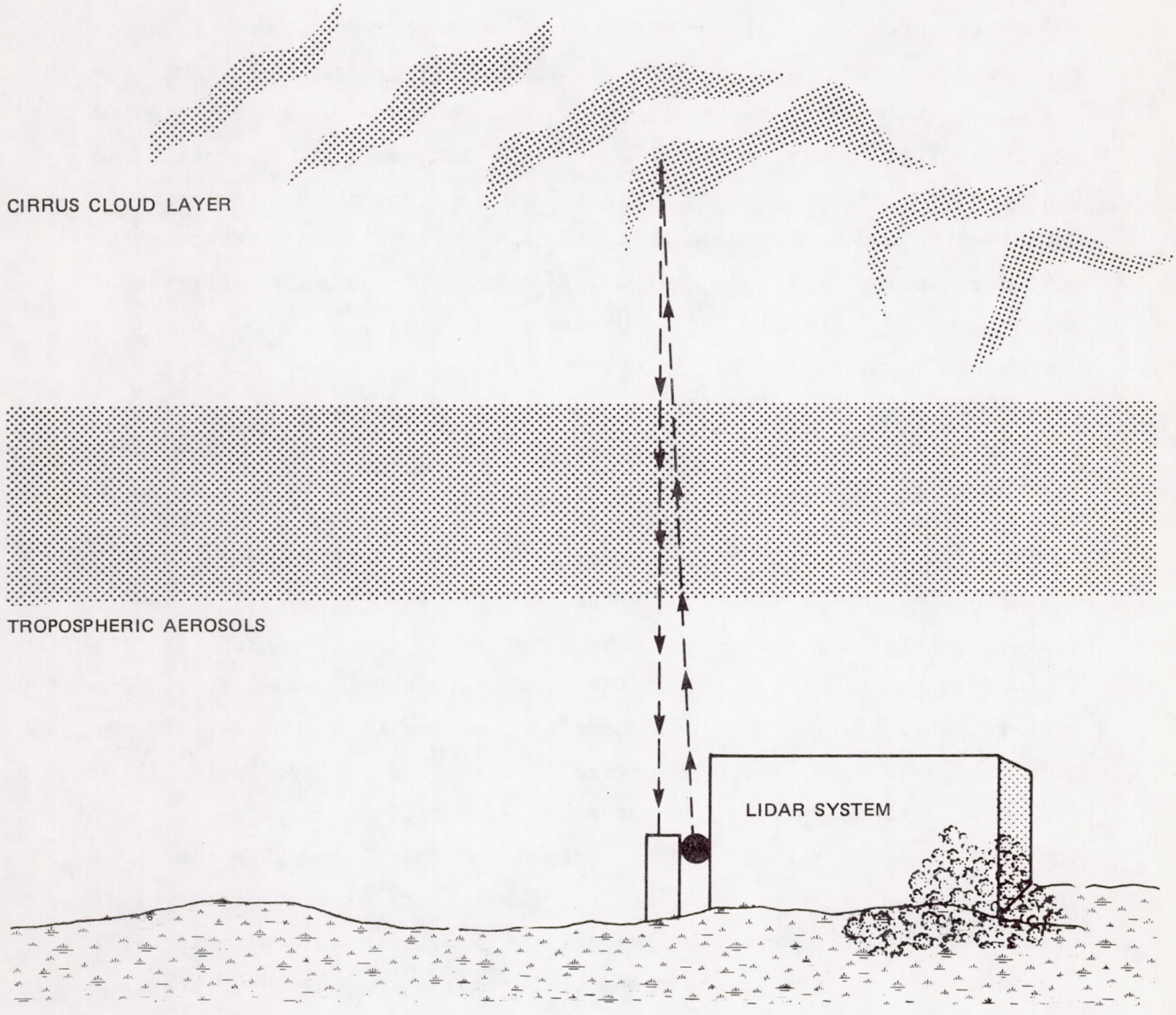

FIGURE 6 PICTORIAL REPRESENTATION OF SIMULTANEOUS CIRRUS/TROPOSPHERIC AEROSOL MEASUREMENT

C. Lidar System Development During Contract

The major emphasis in the previous experimental measurements was to obtain optical signals from the stratospheric aerosol layer, which required the maximum signal and minimum noise performance from the system. Since this was a single-wavelength measurement, a cooled infrared filter was placed ahead of the detector to minimize the background noise level. Since the stratospheric/tropospheric experiments contemplated on this project were multi-wavelength DISC measurements, this fixed band pass filter had to be either eliminated or replaced by a tunable infrared band pass filter. Various ways of achieving tunable cooled filters were examined, but none could be accommodated within the time and funding constraints. Therefore it was decided to operate the detector without a filter even though this lack of filtering would produce a higher noise level for the system.

The major problem encountered in the previous experimental series was thought to be caused by saturation of the preamplifier which follows the infrared detector. Detailed investigation of the preamplifier and the preamplifier/detector combination failed to reveal the saturation problem. Careful investigation showed that the problem was caused by the electrical discharge associated with laser firing and picked up by the detector, preamplifier, and data cable to the data acquisition system. Small changes in the physical configuration of the detector, preamplifier, and/or data cable produced dramatic changes in the effect, thus explaining the intermittent occurrence of the problems seen in the previous experimental series.

An extensive effort was made to shield the detector, preamplifier, and data cable. The preamplifier was enclosed in a separate metal box, and the power supply normally used for the preamplifier was replaced by a battery pack enclosed in the metal cabinet. Double-shielded cables were used from the preamplifier

enclosure to the detector and the data acquisition system. Electrically-isolated mountings were incorporated into the detector housing to eliminate ground loops or additional EMI pickup from the telescope housing itself. These and other modifications reduced the baseline variations to the point were they were not discernible with integration of 100 pulses.

During these tests, it was also observed that other sources of interference also caused difficulties. Local radio stations were initially troublesome, but the increased levels of shielding reduced their contribution to a low level. A more difficult interference source was a high-powered transmitter that is used intermittently to relay data to and from an SRI field site in Alaska. This transmitter is used from a few minutes to a few hours each day and produces very high levels of interference in the system. These signals are still present even with the extensive shielding added to the system, and we were not able to take sufficiently noise-free data when this transmitter was operating. The approximate operating schedule of these transmissions was determined and data runs were scheduled for periods when the transmitter was not supposed to be operating. The schedule was not reliable, however, and unexpected operation of the transmitter caused us to terminate runs prematurely and to miss data acquisition on days when cloud characteristics were favorable.

The principal difficulty encountered in upgrading the CO_2 laser over a wide range of wavelengths was the large variation in power output. When the laser was set up with the normal operating gas mixture, the highest possible output was produced on the normal P20 operating line at 10.6 μ. When tuned over a wide wavelength range, however, the energy output fell to less than 10% of its peak value and was too low to make effective measurements. In order to achieve the maximum tuning range with this laser system, several adjustments of the gas mixture were made in order to operate at wavelengths other than the peak power points of the four major tuning bands of the laser.

These four major tuning bands and the regions of satisfactory operation obtained by these changes in gas mixture are shown in Figure 7. In the normal operation of the laser only a narrow region around the peaks of the four branches would be available for possible operating wavelengths. With a modified gas mixture, eight operating regions covering a wider and more uniformly spaced wavelength range are possible. Strict precautions in using the laser are necessary with this mode of operation because the laser could be destroyed on the first pulse if operation is attempted at a peak wavelengths regions when adjusted for operation under off-peak conditions. Damage occurs because the laser power in the cavity is higher than the wavelength tuning grating will handle. The need for great caution in

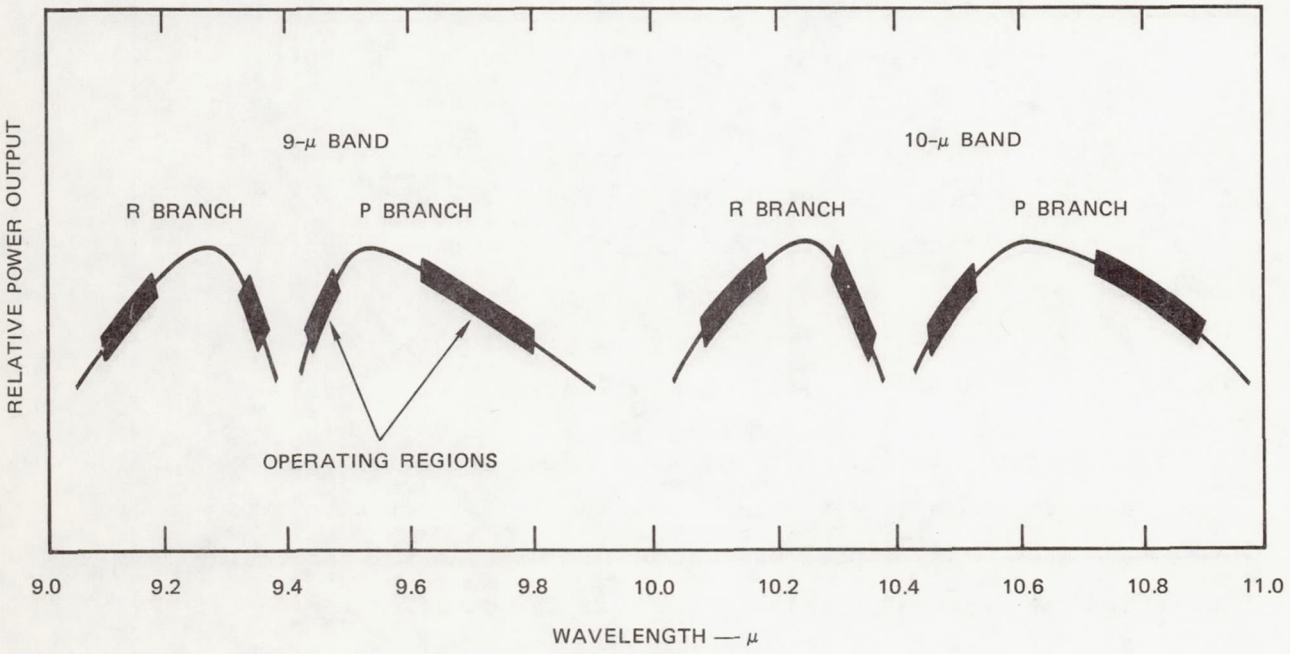

FIGURE 7 THE FOUR MAJOR TUNING BANDS FOR THE CO_2 LASER SYSTEM

tuning the laser precludes the use of shot-by-shot changes in wavelength which are, because of the variability of cirrus clouds, necessary to obtain usable signals. The computer-controlled wavelength tuner is virtually a necessity for shot-to-shot wavelength tuning with a modified gas mixture.

Eight wavelengths were selected for the measurement, one from each of the eight operating regions. In the 9 μ band these wavelengths are P14, P36, R10, and R16, and, in the 10 μ band, P10, P38, R12, and R32. The wavelength selections were dictated primarily by the laser operation and not by the wavelengths that might be optimum for measuring the expected constituents. Further work on multi-wavelength operation of the laser would result in a wider choice of operating wavelengths and could provide more flexibility in providing optimum wavelengths for measurements of particular species.

During initial multi-wavelength operation of the laser, difficulty was encountered with the power measurement apparatus used to monitor the laser power output. This apparatus is normally used to monitor the shot-to-shot power variations occurring in the laser measurement. It was discovered that the power monitoring apparatus had a non-repeatable wavelength dependence and thus did not appear to be an adequate power reference for the measurement. The difficulty was traced to the use of a semi-transparent beam splitter for sampling and attenuating a portion of the transmitted laser beam. The two surfaces of this beam splitter acted as an etalon and thus introduced wavelength variations. No other satisfactory power measuring apparatus was available, and so a search began for other ways of calibrating the laser.

During this time it was also realized that cirrus clouds exhibited a very large pulse-to-pulse variation in backscatter. A number of experimental runs using cirrus clouds as targets showed shot-to-shot power variations of approximately one order of magnitude, with measurements spaced approximately 4s apart. In addition to this short-term variability, changes of two orders of magnitude were

observed over a time scale of approximately 10 min. Even larger variations, including complete disappearance of the signal, were observed during measurements of scattered patches of cirrus clouds. This large variation in scattered signal from the cirrus clouds would introduce large statistical variations in the received signal, and would make detection of the small ratios of backscatter quite difficult.

It became increasingly evident that the wavelength tuner would be necessary in order to reduce the "noise" caused by cirrus reflectivity variations. Unfortunately, the personnel required for completion of the wavelength tuner were not available and thus an alternative solution to this problem was sought. The most satisfactory alternative consistent with the equipment available appeared to be the use of a second laser transmitter operated at a fixed wavelength, and firing just after the highest altitude signal return was received from the variable-wavelength laser. In this way, a pulse-to-pulse calibration for the cirrus backscatter could be made, and the effect of these variations minimized. The second laser was a fixed-wavelength CO_2 laser triggered by a digital delay generator which, in turn, was triggered by the firing of the variable wavelength laser. A block diagram of the two transmitter system is shown in Figure 8.

A representation of the signal return produced by this two laser system is shown in Figure 9. The first part of the signal is due to the firing of the variable-wavelength laser. The tropospheric-aerosol return occurs just after the initial peak and represents the backscattered signal from the lower and middle tropospheric regions. The second peak in the curve occurs as a result of the cirrus cloud signal return at higher altitudes. At a time corresponding to the maximum altitude at which the cirrus clouds are expected, the second major increase in signal occurs from the firing of the fixed-wavelength laser. Backscattered signals from tropospheric aerosols and cirrus clouds are also recorded for this second laser firing.

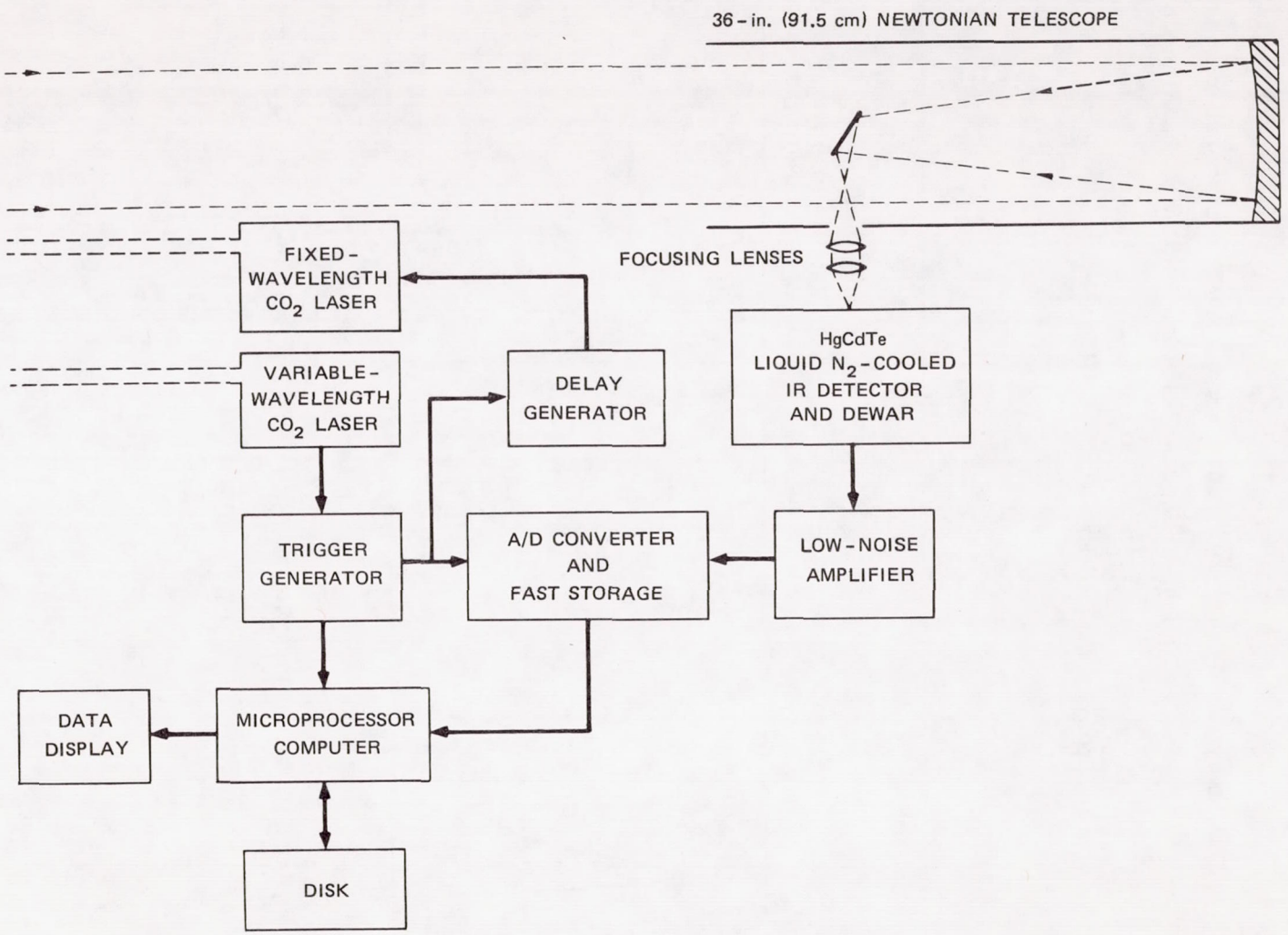

FIGURE 8 EQUIPMENT DIAGRAM FOR THE MODIFIED EXPERIMENTAL INFERRED DISC LIDAR SYSTEM

Each time the variable wavelength laser fires, the entire data period shown in Figure 9 is recorded on disk by the data acquisition system. In this way, a fixed wavelength calibration is obtained for the cirrus backscatter for each shot. The physical layout for the second laser transmitter is shown in Figure 10. This second laser transmitter uses the same receiving optics and detector as the variable wavelength laser. In this way, sensitivity differences due to geometry, detector, or electronics are minimized.

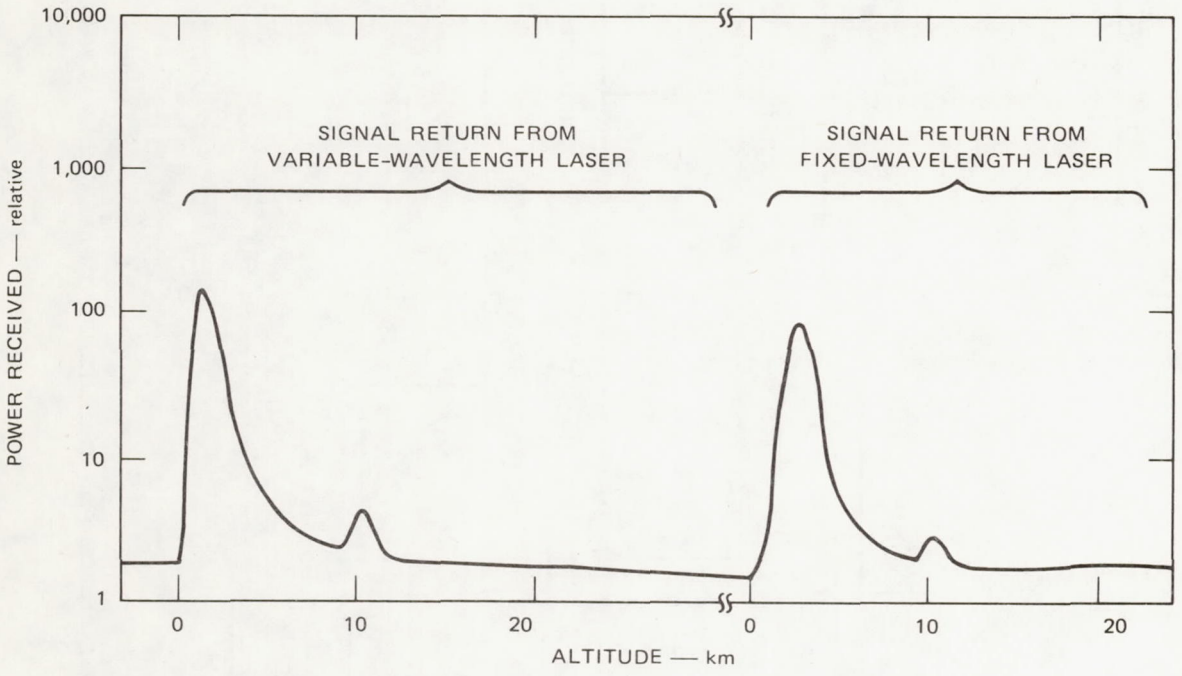

FIGURE 9 REPRESENTATION OF SIGNAL RETURN PRODUCED BY THE TWO-LASER SYSTEM

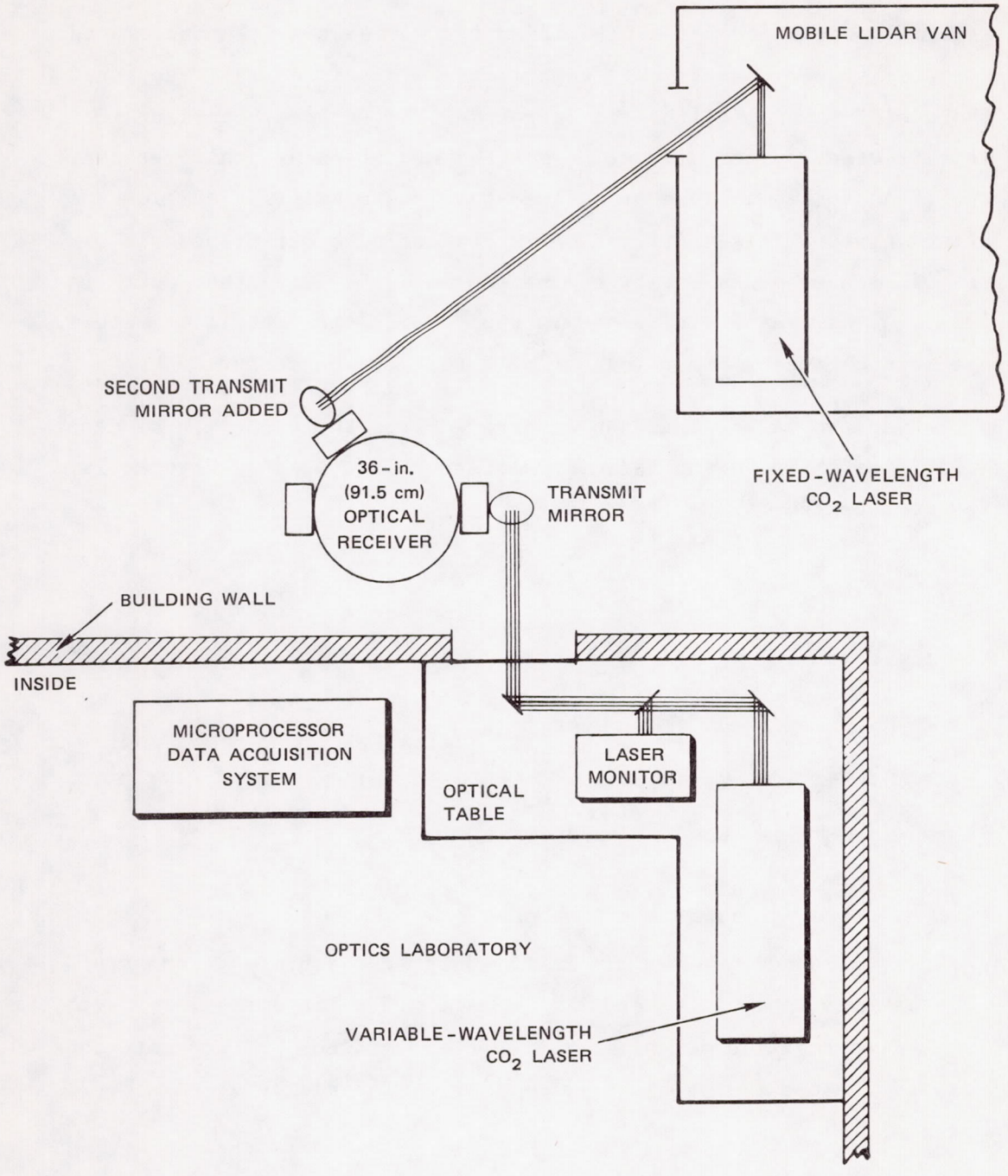

FIGURE 10 PHYSICAL LAYOUT OF THE MODIFIED LIDAR SYSTEM

D. Data Reduction Method

Normal operation of a DISC lidar system assumes a calibrated backscatter (power measurement) capability. This is normally achieved by the use of fixed, calibrated targets. The physical configuration of the present system did not permit the use of such calibrations, however, and forced the use of a fixed-wavelength calibration lidar as an alternative. This modification introduces some differences in the types of measurements that can be made and the way the data is analyzed. The major difference is that backscatter ratios, rather than absolute backscatter values are all that can be measured.

The various ratios that can be derived from the experimental data are clarified by following the nomenclature illustrated in Figure 11. The power received by the lidar system is

$$P_R = G_\lambda P_\lambda \beta_{M\lambda N} \tag{1}$$

where

P_R = received laser power

G_λ = geometry and system coefficient for wavelength λ

P_λ = transmitted power at wavelength λ

β = backscattering coefficient for material M at wavelength λ for shot number N

Figure 11 shows the signals received for two arbitrary shots, X and Y, assumed to be at λ_1 and λ_2. The fixed calibration wavelength is λ_C. Two materials, M_1 and M_2 are assumed to be present and correspond to the tropospheric aerosol layer and cirrus cloud layer, respectively.

One ratio taken in the data processing is the ratio of the variable wavelength signal return to the fixed-wavelength signal return for each shot X or Y. Note that X and Y can be considered either as individual shots or as averages of a series of shots. Since

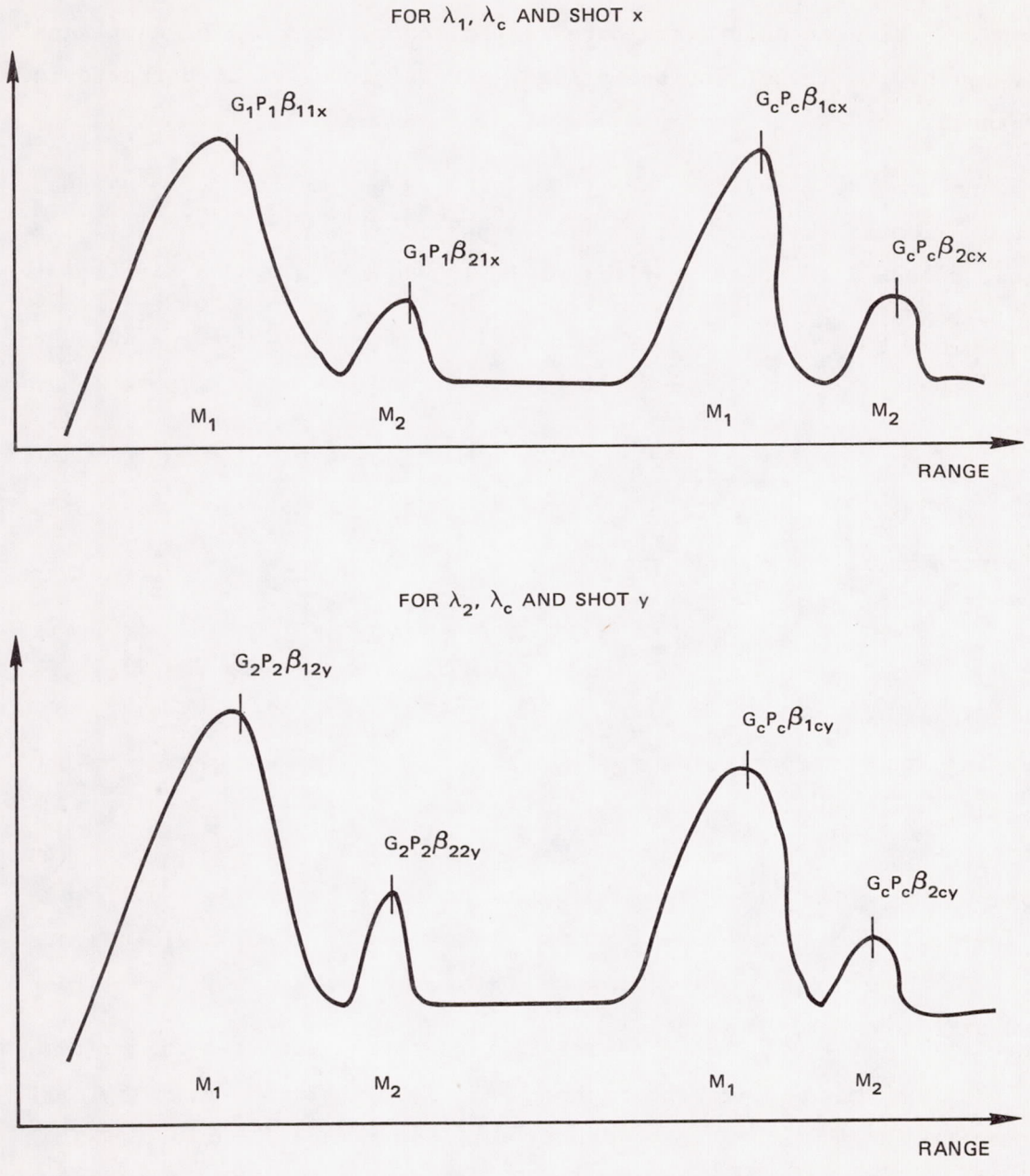

$\beta_{\text{MATERIAL, }\lambda\text{, SHOT NUMBER}}$ = BACKSCATTER COEFFICIENT

$G_\lambda P_\lambda$ = SYSTEM COEFFICIENT

FIGURE 11 NOMENCLATURE FOR SIGNAL PROCESSING

the pulse-to-pulse variation in cirrus backscatter was so high the ratio of variable-wavelength signal to fixed-wavelength signal was normally calculated for each data record (corresponding to a single measurement). These ratios in their general form are illustrated in Figure 12.

Another ratio used in data processing is the ratio of the signal return from the low-altitude (tropospheric) layer divided by the signal return from the high-altitude (cirrus) layer. For a particular wavelength λ_1, and shot X

$$\left.\frac{\bar{R}_{lo}}{\bar{hi}}\right|_x = \frac{\beta_{11x}}{\beta_{21x}} \cdot \frac{\beta_{2cx}}{\beta_{1cx}} \tag{2}$$

This same ratio for λ_2 and shot Y is

$$\left.\frac{\bar{R}_{lo}}{\bar{hi}}\right|_y = \frac{\beta_{12y}}{\beta_{22y}} \cdot \frac{\beta_{2cy}}{\beta_{1cy}} \tag{3}$$

Assuming, on the average,

$$F = \frac{\beta_{2cx}}{\beta_{1cx}} \approx \frac{\beta_{2cy}}{\beta_{1cy}} \tag{4}$$

these ratios give the backscattering ratio for two materials, β_{11x}/β_{21x}, to within the factor F. Note that the geometry and transmitted power factors cancel out in this ratio. This experimentally-measured ratio can be compared with the theoretical ratio for the same materials, and is the final measurement result desired from the experiment.

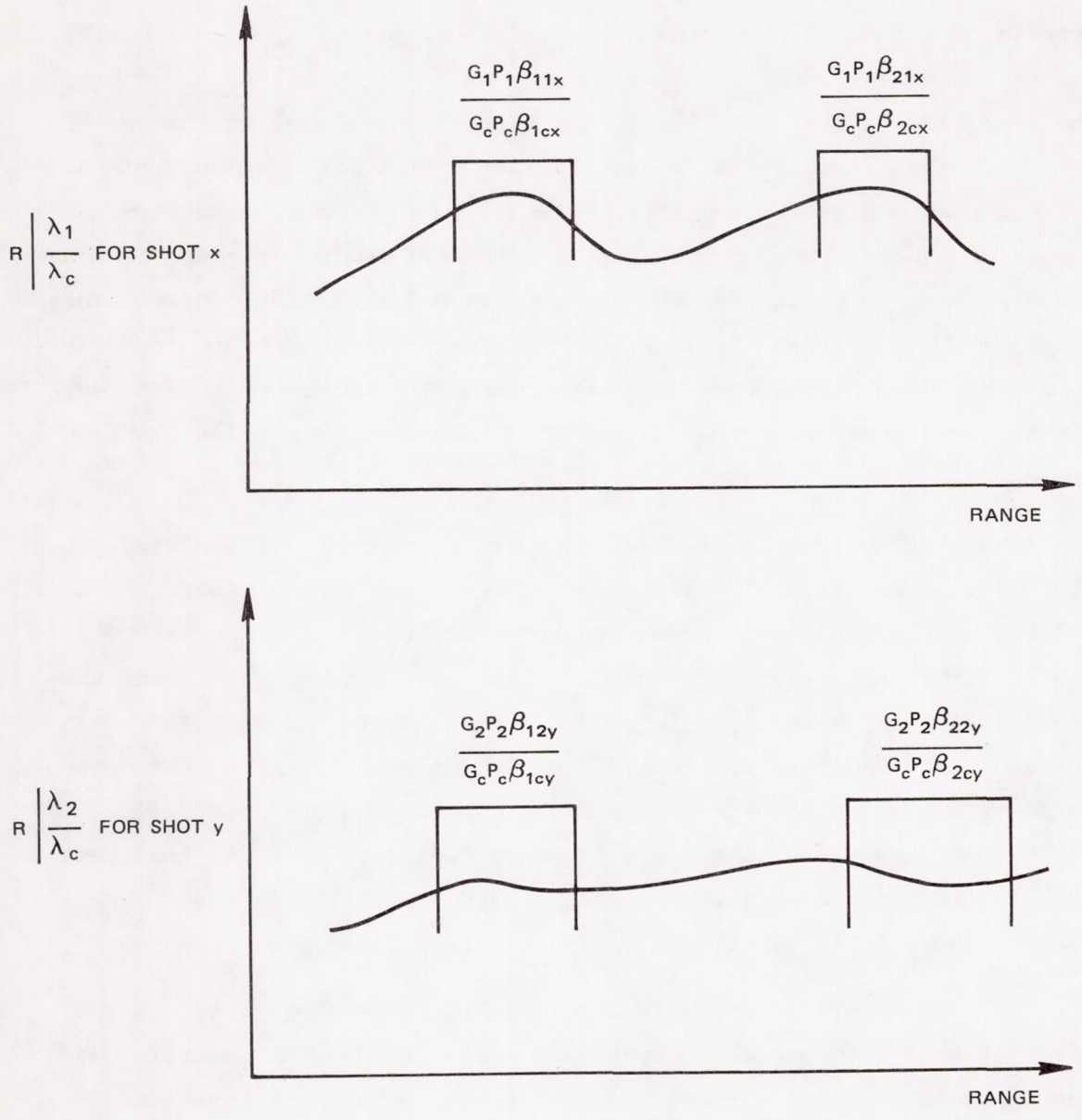

FIGURE 12 NOMENCLATURE FOR RATIO MEASUREMENTS

E. Experimental Results

Several data runs were taken on different days and at different times. Each run would take one to two hours, and all of the runs except one were incomplete because the cirrus clouds disappeared for a portion of the run. Since the laser was tuned manually rather than by computer, measurements were made in groups of 25 to 50 shots, each at the same wavelength. If the cirrus clouds were absent during one or more of these groups the resulting data runs would be incomplete. The run that was considered acceptable apparently had an extensive and continuous haze layer at the same altitude at which cirrus clouds would appear. Thus, when the clouds were not present the haze layer provided a distinct signal return with sufficient SNR to provide acceptable data. The remaining sections will focus on this data run, although information from incomplete runs may be included where appropriate.

The raw uncorrected received power from the cirrus layer is plotted as a function of wavelength in Figure 13. Since there was no reliable method of obtaining an absolute calibration for the laser at each of the operating wavelengths, this curve does not represent the true relative backscatter for the cirrus layer. Comparison with curves described later, which are normalized to the reference wavelength, shows that the raw measurements are not grossly different in overall shape from the corrected measurements. Thus it appears that differences in received signal caused by backscatter are larger than differences in signal due to laser calibration errors.

In order to compensate for the high shot-to-shot signal variability, each variable-wavelength signal return was normalized to the fixed 10.6 μm signal return as described above. Figure 14 shows the results of this normalization process at each of the laser wavelengths. These curves were obtained by normalizing each variable-wavelength laser shot to the received signal at the calibration wavelength. These normalized curves were then averaged

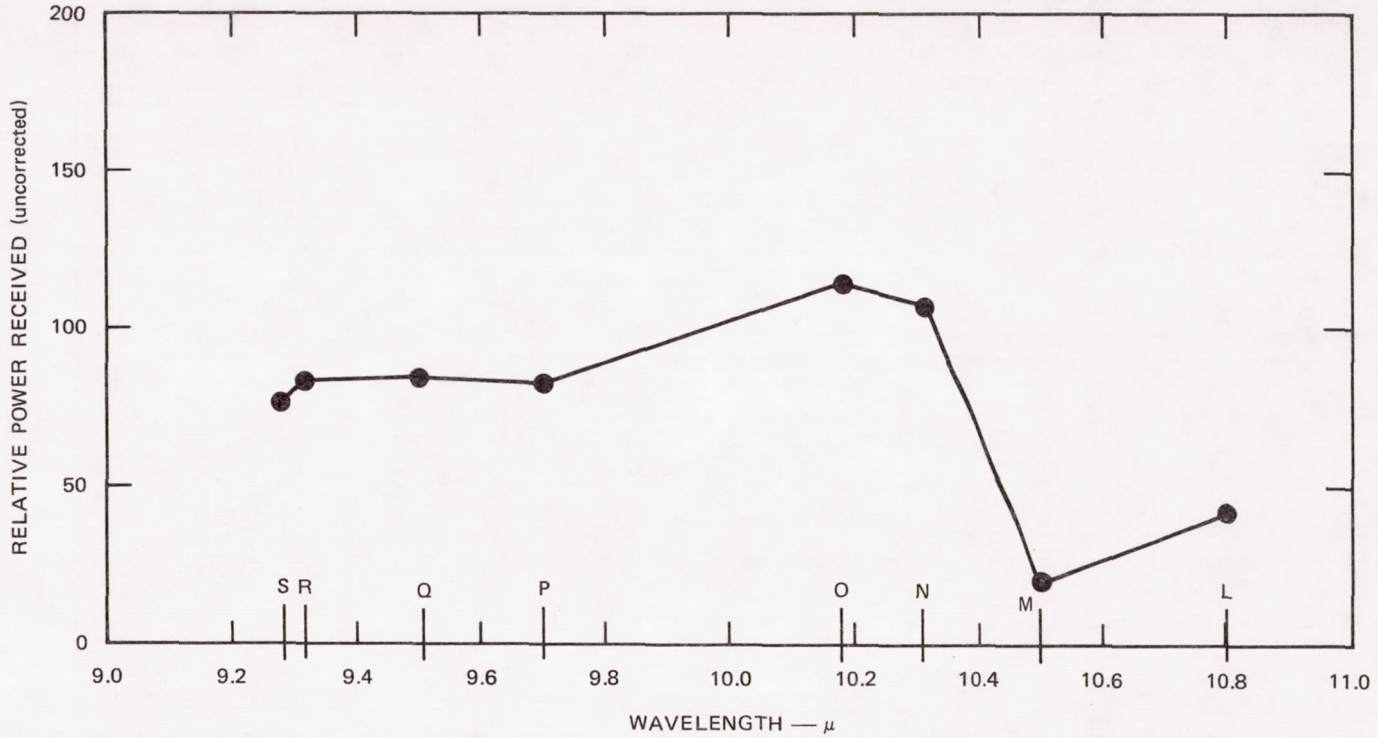

FIGURE 13 UNCORRECTED RECEIVED SIGNALS FROM THE CIRRUS CLOUD LAYER

over the 25 to 50 shots taken at each wavelength and the resulting curves are shown in the figure. The altitudes for the low-and high-altitude measurement points are shown by the tick marks on the horizontal axis of Figure 13. The operating wavelengths are indicated by the letters L through S, respectively, and actual wavelengths of these laser lines are given in Table 3.

Examination of curve L in Figure 14 shows that the normalized signal return from the low-altitude layer is substantially lower than that of the high-altitude layer. Curve M shows that they are approximately equal. Curves N and O indicate that the low-altitude signal return is higher than the high-altitude signal return. Curves P through S show mixed but approximately equal returns from the two layers.

TABLE 3

MEASUREMENT WAVELENGTHS

Letter Code	Line Designation	Wavelength (μm)
L	P(38)	10.79
M	P(10)	10.59
N	R(12)	10.30
O	R(32)	10.17
P	R(36)	9.69
Q	P(14)	9.50
R	R(10)	9.32
S	R(16)	9.29

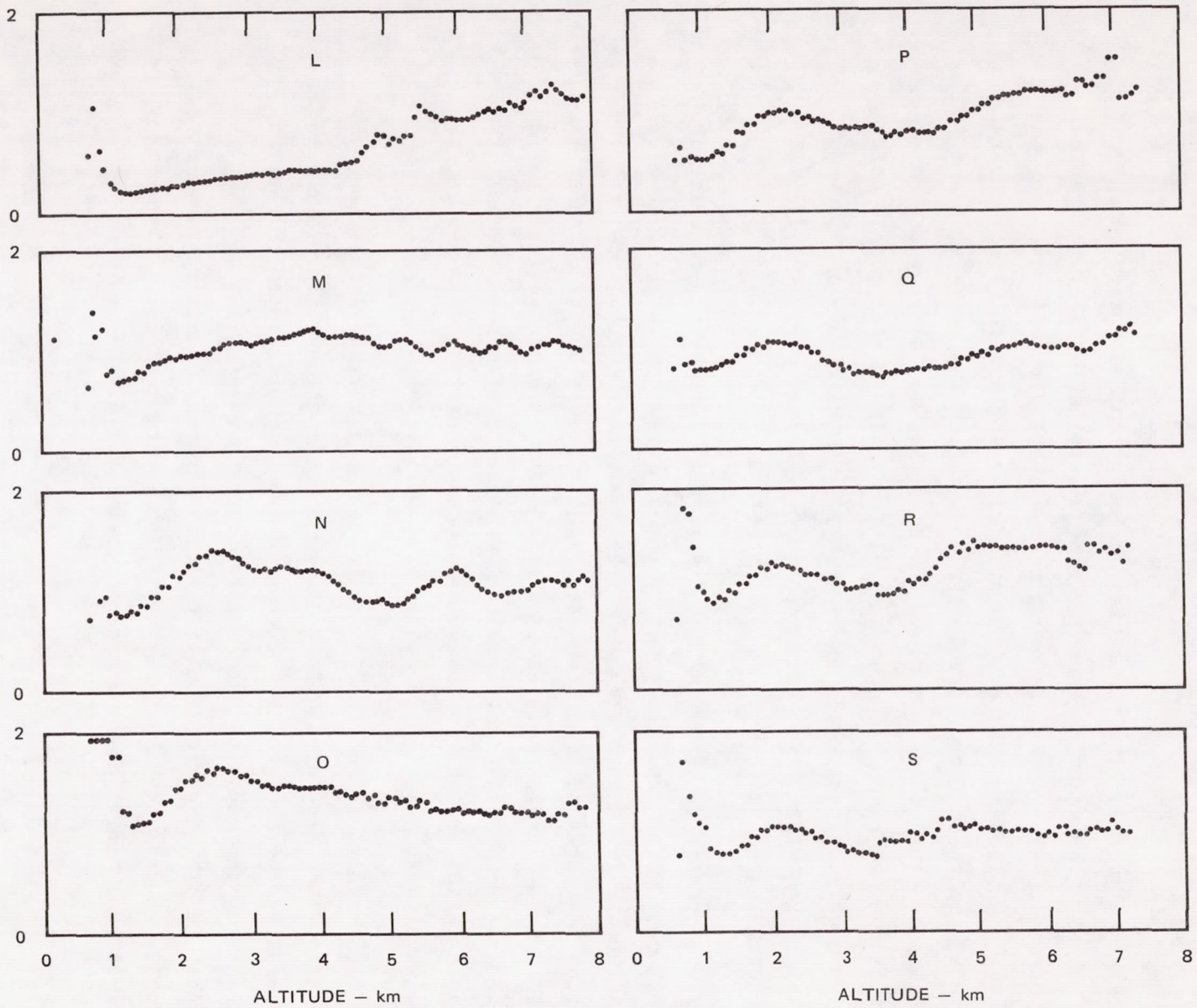

FIGURE 14 SIGNAL RETURN AT EACH MEASUREMENT WAVELENGTH, NORMALIZED TO SIGNAL RETURN AT 10.6 μm

A plot of the ratio of low-altitude to high-altitude normalized signal return is shown in Figure 15. The theoretical backscatter ratio for water and ice is also shown by the dotted curve in this figure, since it seems to be the material pair that best fits the experimental data. The theoretical calculations are based on use of the NASA tropospheric aerosol size distribution. The actual measurement wavelengths are shown by the short vertical bars in the figure. Although the experimental curve follows the same general shape as the theoretical curve, the position of the peak is offset in wavelength. The dashed curve shows the experimental results of a partial run, during which the high altitude clouds disappeared before the run could be completed. These experimental points show somewhat better agreement with the theoretical curve over the limited wavelength range which data is available.

One possible reason for the discrepancy is that the constituents were not water and ice but were composed of other chemical constituents. Figure 16 shows the wavelength-dependence of the ratios of backscattering for several other constituents to that for ice. Constituents not shown on this curve have backscatter ratios that are very different from the measured values. None of the backscattering ratios for these other constituents show a peak at the same wavelength obtained in the experimental results.

A further correction to the experimental results was made by including the calculated effect of atmospheric attenuation between the tropospheric aerosol and the cirrus layer. Applying these corrections results in the modified experimental curve shown in Figure 17. The effect of this correction is to shift the peak location toward a slightly shorter wavelength, thus slightly increasing the discrepancy between the theoretical and experimental results.

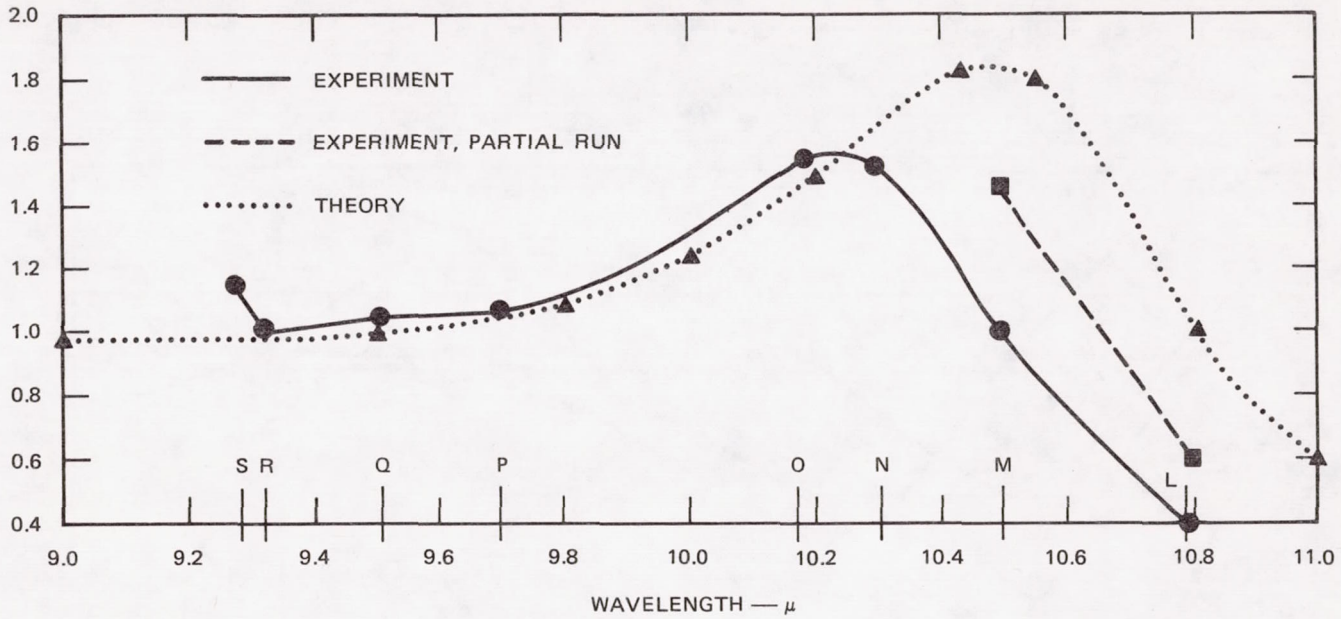

FIGURE 15 A COMPARISON OF BACKSCATTER RATIO FOR EXPERIMENTAL VALUES AND WATER / ICE

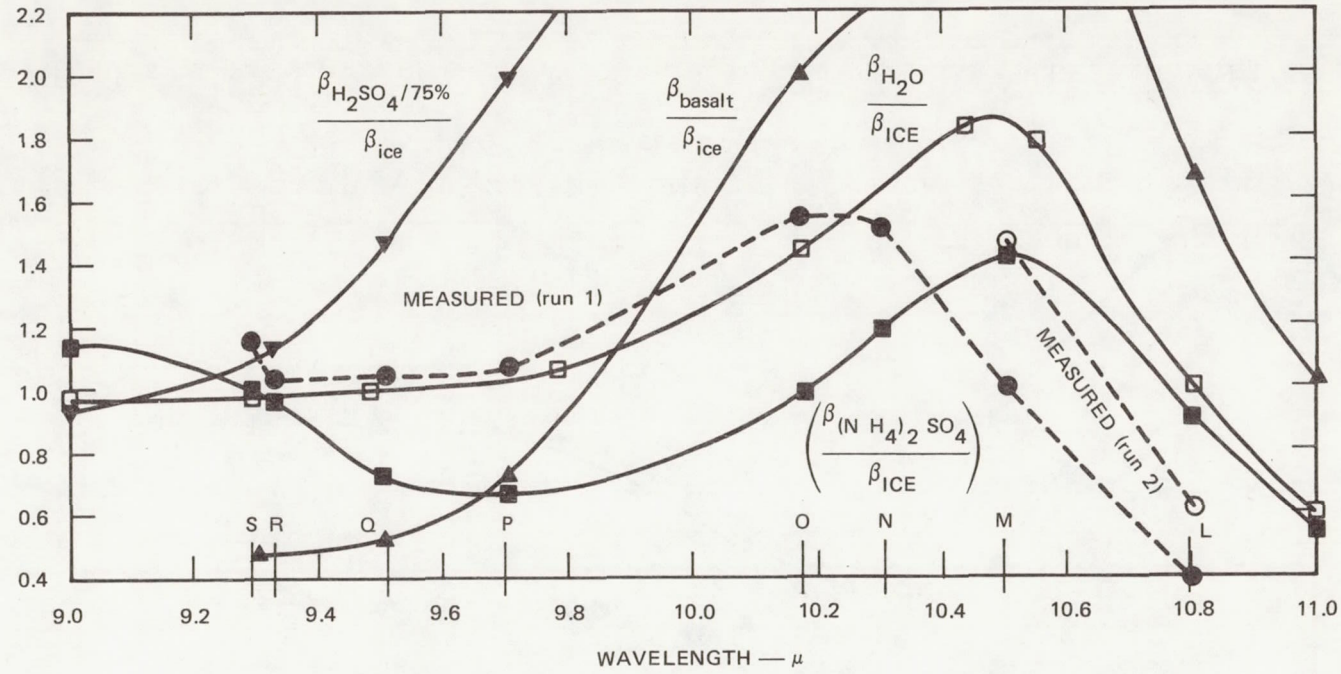

FIGURE 16 A COMPARISON BETWEEN EXPERIMENTAL MEASUREMENTS AND VARIOUS AEROSOL MATERIALS

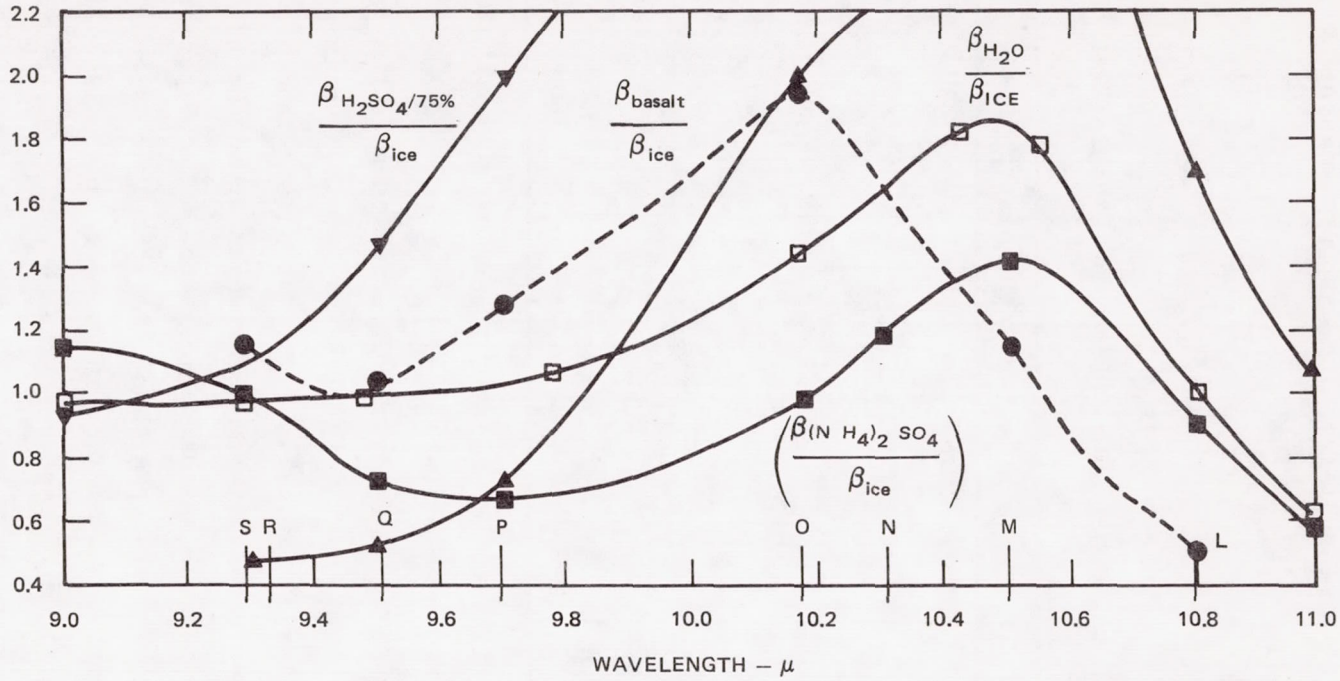

FIGURE 17 EXPERIMENTAL VALUES CORRECTED FOR ATMOSPHERIC ATTENUATION

Another possible reason for the discrepancy is that at very low temperatures, the refractive index of ice changes, in a direction that would make the two peaks coincide more closely. A check with the National Weather Service revealed that the temperature at the altitude where the cirrus clouds were observed was not sufficiently low to account for the observed shift. The data provided by the National Weather Service is included in Table 4.

TABLE 4

METEOROLOGICAL CONDITIONS DURING THE EXPERIMENTAL RUN

Altitude(kft)	Temperature(^{o}c)	Relative Humidity(%)
0	17	74
3	8.6	20
6	3.3	43
9	-1.1	48
12	-6.2	40
15	-12.2	30
18	-17.7	19
21	-24.6	95
24	-30.7	100

Another difficulty concerns slight differences in optical geometry for the two transmitters. Consider the received signal for the lidar system as shown in Figure 9. Starting at the location of lidar system (zero range) the initial rise in the received signal is caused by the gradual overlap of the transmit and receive beam patterns. At the peak they are nearly overlapped and the 1/R range dependence of the signal begins to dominate. The first portion of this decreasing curve represents the received signal from the tropospheric aerosol. Anomalies in the data analysis indicate that there are significant differences in the convergence geometry between the fixed-and variable-wavelength laser beam patterns. Similiar effects have been observed in two-wavelength DIAL systems. These differences in convergence may also be wavelength-dependent and thus introduce errors in the apparent received signal strength for the tropospheric aerosol layers.

Additional difficulties were encountered because of time delay effects between the signals from the two layers. These time-delay effects resulted in an uncertainty of one or two range cells in the position of the fixed-wavelength laser signal return with respect to the variable-wavelength signal return. The method used to resolve the difficulties caused by this time jitter was to completely process all the data with successive adjustments in time delay over a range of plus or minus two range cells from the nominal experimental data. These small differences in timing were found to produce significant changes in the appearance of the normalized data. In particular, large swings in normalized signal amplitude were observed at the leading and trailing edge of aerosol scattering layers. The correct time delay value was chosen by selecting the time delay that produced the smoothest set of curves. These curves are those shown in Figure 14.

F. System Performance Analysis

The signal-to-noise calculation for the original system indicated that an SNR of 94 would result from integration of 1,000 pulses, and an SNR of 30 from integration of 100 pulses. Experimental runs with pulse integrations varying from 100 to 600 pulses failed to reveal a signal from the stratospheric aerosol. Examination of the present system parameters, however, reveals that the laser energy output was reduced from 7 J to 3 J, and the removal of the cooled infrared filter increased the noise from the detector.

A major difference in the operation of the present experiment is the use of shorter range cells in order to resolve the slight peak that would be expected from the stratospheric aerosol layer. Using estimates for the present experimental system parameters yields the SNR values shown in Table 5. It is apparent that compromises in the various system parameters have degraded the system performance to the point where a signal from the stratospheric aerosol layer might not be measurable. It should also be noted that these estimates utilized the

original backscatter estimate that was calculated for the time period shortly after a volcanic eruption. A reduction in backscatter coefficient by a factor of 10 might be more characteristic of stratospheric aerosols in the absence of a volcanic eruption. If such a low backscatter coefficient is actually the case, a signal from the stratospheric aerosol layer would not be measurable with the present experimental system.

TABLE 5

SNR FOR THE PRESENT EXPERIMENTAL SYSTEM

Range Resolution (km)	SNR
1	.63
2	.88
3	1.4

The system parameters appropriate for an advanced space shuttle lidar system are given in Table 6. This system would have a SNR of 11.9 for integration of 1,000 shots, based on the original backscatter coefficient for volcanic conditions. This system would be marginal (SNR approximately equal to 1) for a reduction in backscatter of 10, as might be appropriate to non-volcanic conditions. Backscatter from tropospheric aerosols and thin cirrus is at least 200 times larger than the backscatter from stratospheric aerosols, and thus these targets could be measured using the space shuttle system.

The pulse energy of the space shuttle lidar was assumed to be limited to 100 J because of the large primary power requirements necessary to run large laser systems. Larger CO_2 laser systems are commercially available and have power outputs in the 200 - to - 1,000 J range. Such systems are only a few percent efficient, however, and could require more than 20KW of primary power for operation. Substained operation with such power requirements was not deemed feasible for this application.

TABLE 6

PARAMETERS OF THE SPACE SHUTTLE LIDAR SYSTEM

Transmitter:	
Type of Laser	CO_2
Transmitted Energy	100 J
Pulse Width	1 μs
Beam Divergence	1 mr
Expected Pulse-Repetition Frequency (PRF)	0.1 Hz (repetitive) 10 Hz (burst mode)
Tunable Wavelength Range	9-11 μm
Receiver:	
Telescope Diameter	36 in.
Field of View	1.2 mr
Detector Sensitivity	2×10^{11} cm $Hz^{1/2}/W$
Detector Size	10^{-3} cm^2
Filter Type	cooled, variable-wavelength
Filter Bandwidth	1%

III CONCLUSIONS

Backscattered signals from cirrus clouds and tropospheric aerosols were found to have sufficient SNR to permit differential-scatter spectral measurements to be made. The experimentally-observed backscattering ratios appeared to be closest to the calculated backscattering ratios for water and ice, although these were not the materials expected. The reason for this discrepancy may be due to a mixture of materials in the tropospheric aerosols, the effects of non-spherical particles, or other effects not studied as part of this contract effort. Refractive indices for mixtures of constituents were not available and thus prevented theoretical calculations of scattering spectra for these mixtures. It is quite possible that a mixture of materials may produce spectra that are closer to the experimentally-observed values.

Some method for calibrating the absolute received power level is needed for this system, such as a telescope mounting that would permit tilting down from the vertical so that a calibrated reflector could be brought into the field of view. Even so, a second laser operating at a fixed wavelength may be needed to provide a correction if cirrus clouds or other targets with highly variable scattering are observed.

An analysis of the sensitivity expected with the present experimental lidar system shows that it will be difficult to detect stratospheric aerosol returns. Using a 100 J laser, a lidar system for the space shuttle would be capable of seeing tropospheric aerosols and subvisible cirrus clouds, but would be of marginal utility for stratospheric aerosols during non-volcanic times unless larger lasers are used.

It is recommended that further theoretical and experimental investigations of the scattering properties of aerosols be made before additional outdoor long-range experiments are undertaken. The present experimental series has shown the feasibility of measuring differential backscattering spectra, but the existing theoretical data base appears to be inadequate for identifying the experimentally-measured spectra.

REFERENCES

1. D. S. Colburn and J. B. Pollack, "Infrared Backscatter Spectra for Differentiation of Stratospheric Aerosol Composition," presented at the Seventh International Laser Radar Conference, SRI International, Menlo Park, California, November 4-7, 1975.

2. R. O. Duda and P. E. Hart, Pattern Classification and Scene Analysis (John Wiley & Sons, Inc., New York, N.Y., 1973).

3. M. L. Wright and G. Johnson, "Lidar Determination of the Composition of Atmospheric Aerosols," Interim Technical Report, Contract NAS2-8914, SRI Project 4358, Menlo Park, California, (December 1977).